

# Preliminary measurement of $\mathcal{B}(\tau^- \rightarrow K^-\pi^0\nu_\tau)$ using the *BABAR* detector

F. Salvatore<sup>a</sup> and A. J. Lyon<sup>b</sup>

*for the BABAR Collaboration*

<sup>a</sup>Royal Holloway College, University of London, Egham, Surrey,  
TW20 0EX, United Kingdom

<sup>b</sup>University of Manchester, Manchester, M13 9PL, United Kingdom

A preliminary measurement of the branching fraction  $\mathcal{B}(\tau^- \rightarrow K^-\pi^0\nu_\tau)$  is made using  $124.4\text{ fb}^{-1}$  of  $e^+e^-$  collision data provided by the PEP-II accelerator, operating primarily at  $\sqrt{s} = 10.58\text{ GeV}$ , and recorded using the *BABAR* detector. We measure:  $\mathcal{B}(\tau^- \rightarrow K^-\pi^0\nu_\tau) = (0.438 \pm 0.004\text{ (stat)} \pm 0.022\text{ (syst)})\%$ . This result is the world's most precise measurement of this branching fraction to date and is consistent with the world average.

## 1. INTRODUCTION

Hadronic (semileptonic)  $\tau$  decays provide a clean laboratory for studying the hadronic weak current. This is because there is no evidence to suggest that the  $\tau$  lepton has substructure and it is the only lepton sufficiently massive to decay into hadrons. Hadronic products from  $\tau$  decays give access to the light quark vector ( $V$ ) and axial-vector ( $A$ ) spectral functions, which give insight into the dynamics of QCD at intermediate scales as well as provide tests of the Standard Model itself. Decays of the  $\tau$  lepton are therefore important in determining the charged hadron decay constants and spectral functions. For decays with overall net strangeness,  $SU(3)_f$  symmetry breaking can be used to determine the Cabibbo-Kobayashi-Maskawa (CKM) matrix element magnitude  $|V_{us}|$ , the strong coupling constant,  $\alpha_s$ , and the strange quark mass,  $m_s$  [1]. Direct measurements of the Cabibbo angle ( $\theta_c$ ) are therefore possible from strange hadronic  $\tau$  decays. These are all tests of the Standard Model and deviations from predicted values would indicate exciting new physics.

Hadrons from  $\tau$  decays are produced via  $W$  emission. Relative to non-strange ( $ud$ ) currents, strange ( $us$ ) currents of  $\tau$  decays are suppressed by an amount  $(|V_{us}|/|V_{ud}|)^2 \simeq \tan^2 \theta_c$ , where  $|V_{ud}|$  and  $|V_{us}|$  are the absolute values of the

CKM matrix elements. Resonant decay dominates these currents: the strange vector current is dominated by a  $K^*$  resonance which decays to  $K\pi$  and the strange axial-vector current by the  $K_1$  which decays mostly via  $K\rho$  and  $K^*\pi$  to  $K\pi\pi$ .

The high luminosity provided by the PEP-II accelerator, coupled with a  $0.89\text{ nb}$   $\tau^+\tau^-$  production cross-section near the operating energy of  $\sqrt{s} = 10.58\text{ GeV}$ , provides a high statistics sample with which to study the strange hadronic decay  $\tau^- \rightarrow K^-\pi^0\nu_\tau$  using the *BABAR* detector. In recent years, measurements of  $\tau$  decay branching fractions to strange hadronic final states and studies of the strange spectral functions have been conducted by ALEPH [2], CLEO [3] and OPAL [4], but have often been limited by statistics. Significant improvements in precision are expected from *BABAR* results due to the higher statistics data sample available.

## 2. THE BABAR DETECTOR AND DATA SET

The *BABAR* detector is described in detail in [5]. Charged particles are detected and their momenta measured with a 5-layer double sided silicon vertex tracker (SVT) and a 40-layer drift chamber (DCH) inside a 1.5 T superconducting solenoidal magnet. A ring-imaging Cherenkov detector (DIRC) is used for the identification of

charged particles. Energies of neutral particles are measured by an electromagnetic calorimeter (EMC) composed of 6,580 CsI(Tl) crystals, and the instrumented magnetic flux return (IFR) is used to identify muons.

The analysis described in this paper is based on the Run 1+2+3 data set taken using the *BABAR* detector at the PEP-II linear collider [6] located at SLAC in the data-taking periods between October 1999 to June 2003. During this period a total of  $124.4\text{ fb}^{-1}$  of data was recorded:  $112.3\text{ fb}^{-1}$  at  $\sqrt{s} = 10.58\text{ GeV}$  and  $12.1\text{ fb}^{-1}$  at  $\sqrt{s} = 10.54\text{ GeV}$ . With an expected cross-section for  $\tau^+\tau^-$  pair production of  $(0.89 \pm 0.02)\text{ nb}$  at the luminosity-weighted  $\sqrt{s}$ , this data sample contains over 200 million  $\tau$  decays.

Monte Carlo (MC) studies of simulated signal and background events were carried out using various MC samples. The  $\tau$  MC events studied were generated with KK2f [7] and decayed with TAUOLA [8] using  $\tau$  branching fractions based on PDG 2002 [9]. In the MC, the  $\tau^-$  decays to  $K^-\pi^0$  via the  $K^*(892)^-$  resonance with a branching fraction of 0.46%. Non- $\tau$  hadronic and dilepton MC samples are used for studying the non- $\tau$  backgrounds.

The MC samples are combined by scaling to the data luminosity, using their relative cross-sections at *BABAR*.

### 3. SELECTING $\tau^- \rightarrow K^-\pi^0\nu_\tau$ EVENTS

The event is divided into two hemispheres in the centre-of-momentum system (CMS) using the plane perpendicular to the thrust axis, which is the direction which maximises the sum of the longitudinal momenta of the neutrals and tracks in the event. The number of tracks in each hemisphere is used to define the topology of the event. Events with one charged track in each hemisphere pointing towards the interaction point are classified as a 1-1 topology. These are used in this analysis.

Additional cuts are imposed to further reduce the backgrounds. The net charge of the event is required to be zero and a cut on the thrust magnitude of the event,  $|\text{thrust}| \geq 0.9$ , is imposed to reduce the non- $\tau$  background.  $B\overline{B}$  and con-

tinuum events are further rejected by requiring that the ratio of the 2<sup>nd</sup> to the 0<sup>th</sup> Fox-Wolfram moment,  $R_2$ , is  $R_2 \geq 0.5$ .

One signature of  $\tau$  decays is the presence of missing momentum in the event due to the neutrinos that escape detection; a minimum cut on the total missing momentum in the CMS of the event,  $P_{miss}$ , is applied in order to reject background coming from continuum and Bhabha events, where very little missing momentum is expected:  $P_{miss} \geq 0.5\text{ GeV}/c$ .

Events where both charged tracks are identified as electrons are rejected. Moreover, only events with exactly one  $\pi^0$  and with no identified  $K_s^0$ s are retained. Electrons are identified using the ratio of calorimeter energy to the track momentum ( $E/p$ ), the ionisation loss in the tracking system ( $dE/dx$ ) and the shape of the shower in the calorimeter.  $\pi^0$ s are identified by combining pairs of energy deposits of more than 50 MeV that are not associated with any charged particle candidates. Only  $\pi^0$ s reconstructed from two separate neutral energy deposits are considered in this analysis. An additional cut on the lateral shape of the electromagnetic shower (manifest as neutral energy clusters) is used to reject fake neutral candidates arising from noisy channels in the EMC.

Only events with one charged track identified as a kaon are considered in the analysis. Kaons are identified using the ionisation loss in the tracking systems ( $dE/dx$ ) and from the information obtained from the DIRC. The efficiency of this selection for data ( $\varepsilon_{\text{data}}$ ) and MC ( $\varepsilon_{\text{MC}}$ ) as a function of the track momentum has been studied using control samples of  $D^{*\pm} \rightarrow D^0\pi^\pm$ ,  $D^0 \rightarrow K\pi$  events. The MC efficiency for the kaon selection obtained in this analysis is then corrected by the ratio  $\varepsilon_{\text{data}}/\varepsilon_{\text{MC}}$  in order to take into account possible differences. The procedure is explained later in Section 4, whilst the associated systematic error is discussed in Section 5.

Once the kaon is selected, only events in which the  $\pi^0$  candidate form an angle  $\theta_{K\pi^0} \leq 1.0\text{ rad}$  with the kaon track in the CMS are considered.

Approximately 35% of  $\tau$  decays are to fully leptonic final states. Requiring that the track in the hemisphere opposite to the kaon candidate

is identified as an electron or muon (“tagging”) strongly reduces the hadronic backgrounds. In this analysis, a lepton tag is defined as the condition that the non-signal-side track is identified as an electron or muon. Muons are identified by hits in the IFR and small energy deposits in the calorimeter.

A significant component of the background to the  $\tau^- \rightarrow K^-\pi^0\nu_\tau$  decay channel comes from hadronic  $\tau$  decays to one charged kaon and two or more  $\pi^0$ s, in which only one  $\pi^0$  is correctly identified and there is one or more additional neutral cluster in the signal hemisphere. In order to reject such events, a cut on the total energy that is unassociated to any charged track or the  $\pi^0$  in the signal region,  $E_{unass}^{SigHemi} \leq 50\text{ MeV}$ , is applied.

The overall signal efficiency is given by:

$$\varepsilon_{\text{sig}} = \frac{N_{\text{sig}}^{\text{sel}}}{N_{\text{sig}}^{\text{gen}}}, \quad (1)$$

where  $N_{\text{sig}}^{\text{gen}}$  is the number of generated signal events and  $N_{\text{sig}}^{\text{sel}}$  is the number of selected signal events. A total of  $1.442 \times 10^6 \tau^- \rightarrow K^-\pi^0\nu_\tau$  signal events were generated, i.e. where one  $\tau$  decays to the signal mode and the other  $\tau$  decays into any of the allowed  $\tau$  decay modes. The statistical uncertainty associated with the signal efficiency, as predicted by the Monte Carlo, is given by:

$$\sigma_\varepsilon = \sqrt{\frac{N_{\text{sig}}^{\text{sel}} N_{\text{sig}}^{\overline{\text{sel}}}}{(N_{\text{sig}}^{\text{sel}} + N_{\text{sig}}^{\overline{\text{sel}}})^3}}, \quad (2)$$

where  $N_{\text{sig}}^{\overline{\text{sel}}} = N_{\text{sig}}^{\text{gen}} - N_{\text{sig}}^{\text{sel}}$ <sup>1</sup>.

The total  $\tau^- \rightarrow K^-\pi^0\nu_\tau$  selection efficiency, which includes the efficiency corrections that are described in Section 4, is  $(0.92 \pm 0.01)\%$ ,  $(0.69 \pm 0.01)\%$  and  $(1.61 \pm 0.01)\%$  for the  $e$ -tag,  $\mu$ -tag and combined samples respectively.

#### 4. EFFICIENCY CORRECTIONS

Since imperfect detector simulation may mean that the reconstruction/selection efficiencies differ between real and Monte Carlo data, some efficiency corrections are applied to the Monte Carlo data.

<sup>1</sup>No luminosity scaling nor efficiency corrections are applied to  $N_{\text{sig}}^{\text{gen}}$ ,  $N_{\text{sig}}^{\text{sel}}$  and  $N_{\text{sig}}^{\overline{\text{sel}}}$ .

A detailed study of the  $\pi^0$  efficiency has been carried out.  $\tau^\pm \rightarrow \rho^\pm\nu_\tau$  and  $\tau^\pm \rightarrow \pi^\pm\nu_\tau$  decays were used to study the  $\pi^0$  efficiency for real and Monte Carlo data. As a result of this study, a per  $\pi^0$  momentum-independent data/MC efficiency correction of  $\varepsilon_{\text{neu}} = 0.981$  should be applied to the MC, i.e. corresponding to a weight of 1 applied to the real data. Since only one  $\pi^0$  is selected in this analysis the MC is weighted with 0.981 as a  $\pi^0$  efficiency correction.

A momentum-independent data/MC correction of 0.5% per track is applied, leading to a total data/MC tracking efficiency correction of 0.990.

The performances of the selectors used for particle identification (PID) differ between real data and Monte Carlo data and so efficiency corrections to correct the Monte Carlo data to the real data are applied. For each PID selector, a set of efficiency tables (“PID tables”) are used in order to obtain the necessary weights to use to correct the Monte Carlo events. The efficiency correction (data/MC relative efficiency) and corresponding uncertainty is calculated for each track by doing a bin-by-bin comparison with the PID efficiency correction tables for the PID selectors used. The average values obtained for the  $e$ -tag,  $\mu$ -tag and combined samples are 0.968, 0.870 and 0.923 respectively.

The total data/MC efficiency correction,  $\varepsilon_{\text{corr}}$ , is made by combining the efficiency corrections described above.  $\varepsilon_{\text{corr}}$  is used to weight the MC and the average values obtained are 94.0%, 84.5% and 89.6% for the  $e$ -tag,  $\mu$ -tag and combined samples respectively. The systematic error coming from this procedure is described in Section 5.

#### 5. SYSTEMATIC UNCERTAINTIES

Multiplicative uncertainties affect how the observed signal yields are translated into branching fraction measurements.

The total systematic error due to the  $\pi^0$  selection efficiency is 3.26%.

The tracking efficiency is susceptible to bias caused by physics data and MC simulation discrepancies. Almost all the charged tracks identified in this analysis have transverse momenta  $p_T > 0.2\text{ GeV}/c$ . A systematic error of  $\pm 0.7\%$  per

track is assigned for tracks in this  $p_T$  range. Each event contains two reconstructed charged tracks with correlated uncertainties, leading to a total tracking efficiency systematic of  $\pm 1.4\%$ .

The total particle identification systematic that arises from the efficiency correction procedure described in Section 4 for each of the  $e$ -tag,  $\mu$ -tag and combined samples is estimated to be 2.2%, 3.5% and 2.4% respectively.

The relative uncertainty associated with the  $\tau^+ \tau^-$  pair production cross-section is 2.2% and is correlated with the luminosity determination relative uncertainty of 1.2%. Accounting for the correlation, a value of 2.3% is adopted.

The systematic due to signal Monte Carlo statistics is calculated by dividing Eq. (2) by Eq. (1). This is found to be 0.87% for the  $e$ -tag, 1.00% for the  $\mu$ -tag and 0.63% for the combined samples respectively. The systematic error on the background Monte Carlo statistics is 0.83% for  $e$ -tag, 0.97% for  $\mu$ -tag and 0.63% for the combined sample.

Since a number of  $\tau$  decay modes have not yet been precisely measured, particularly those modes which contain Cabibbo suppression factors, the branching fraction used as input to the Monte Carlo comes with a significant uncertainty which feeds into the total systematic uncertainty. In order to evaluate this systematic, a weighted-sum of the  $\tau$  backgrounds is constructed using the Monte Carlo truth for  $\tau$  Monte Carlo events passing the analysis selection criteria. The uncertainties for each background mode are taken from PDG 2002 [9]. The overall estimated uncertainty due to the  $\tau$  backgrounds is given by:

$$\Delta^{\tau-\text{bkg}} = \sqrt{\sum_i \left( w_i \frac{\sigma_i^{\text{PDG}}}{B_i^{\text{PDG}}} \right)^2}, \quad (3)$$

where  $w_i$  is the fraction of events of type mode  $i$  in the total number of  $\tau$  events,  $B_i^{\text{PDG}}$  is the branching fraction and  $\sigma_i^{\text{PDG}}$  is the uncertainty of decay mode  $i$  from PDG 2002.

Table 1 shows the weights and uncertainties of the  $\tau$  background modes remaining in the selected  $\tau^- \rightarrow K^- \pi^0 \nu_\tau$  sample. The resulting systematic uncertainty ( $\Delta^{\tau-\text{bkg}}$ ) attributed to the  $\tau$  background modes is estimated as 0.90% and is

consistent between each of the tagged samples. This error also contains a 0.3% contribution due to the uncertainty on the kaon misidentification rate in all channels containing a charged pion.

Table 1

$\tau$  background uncertainties from PDG 2002 [9] and their weights in the selected  $\tau^- \rightarrow K^- \pi^0 \nu_\tau$  sample.

Decay channel	$w/10^{-2}$	$\frac{\sigma^{\text{PDG}}}{B^{\text{PDG}}} [\%]$
$\tau^- \rightarrow e^- \bar{\nu}_e \nu_\tau$	0.159	0.34
$\tau^- \rightarrow \mu^- \bar{\nu}_\mu \nu_\tau$	0.020	0.35
$\tau^- \rightarrow \pi^- \nu_\tau$	0.062	0.99
$\tau^- \rightarrow \pi^- \pi^0 \nu_\tau$	20.063	0.55
$\tau^- \rightarrow a_1^- \nu_\tau$	0.426	1.10
$\tau^- \rightarrow K^- \nu_\tau$	0.264	3.35
$\tau^- \rightarrow K^{*-} \nu_\tau$ (non-sig)	0.821	4.49
$\tau^- \rightarrow 2\pi^- \pi^0 \pi^+ \nu_\tau$	0.060	2.05
$\tau^- \rightarrow 3\pi^0 \pi^- \nu_\tau$	0.003	9.30
$\tau^- \rightarrow K^- \pi^- K^+ \nu_\tau$	0.009	9.14
$\tau^- \rightarrow K^- K^0 \pi^0 \nu_\tau$	4.456	12.90
$\tau^- \rightarrow K^- \pi^0 \pi^0 \nu_\tau$	0.791	39.70
$\tau^- \rightarrow K^- \pi^- \pi^+ \nu_\tau$	0.010	15.15
$\tau^- \rightarrow \pi^- \bar{K}^0 \pi^0 \nu_\tau$	0.029	11.11
$\tau^- \rightarrow \eta \pi^- \pi^0 \nu_\tau$	0.003	13.79
$\tau^- \rightarrow K^- K^0 \nu_\tau$	0.338	10.38

The total multiplicative systematic uncertainty is the quadrature sum of the individual sources described above and corresponds to 5.0%, 5.7% and 5.0% for the  $e$ -tag,  $\mu$ -tag and combined samples respectively.

## 6. BRANCHING FRACTION MEASUREMENT: $\mathcal{B}(\tau^- \rightarrow K^- \pi^0 \nu_\tau)$

Figure 1 shows the invariant mass spectrum of the selected data and MC  $K^\pm \pi^0$  candidates in the combined ( $e$ -tag+ $\mu$ -tag) sample after all the analysis requirements, including efficiency corrections. In this plot, the signal MC sample is scaled using the branching fraction used in the MC generation:  $\mathcal{B}(\tau^- \rightarrow K^- \pi^0 \nu_\tau) = 0.46\%$ .

The final result for  $\mathcal{B}(\tau^- \rightarrow K^- \pi^0 \nu_\tau)$  is estimated using this sample, where the total number

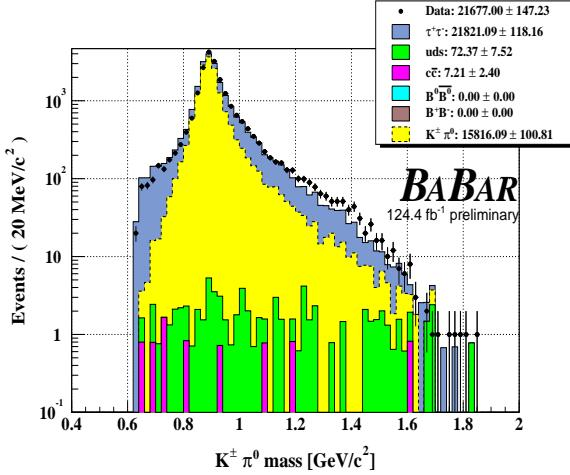


Figure 1. Reconstructed  $K^\pm\pi^0$  mass after selection and efficiency corrections for the combined ( $e$ -tag+ $\mu$ -tag) sample.

of events observed, estimated background level and efficiency are linear superpositions of the two tagged samples (i.e.  $e$ -tag+ $\mu$ -tag) used. As a cross-check,  $\mathcal{B}(\tau^- \rightarrow K^-\pi^0\nu_\tau)$  is calculated for each tagged sample separately and the results obtained are in agreement with the combined result.

The branching fraction  $\mathcal{B}(\tau^- \rightarrow K^-\pi^0\nu_\tau)$  is given by:

$$\mathcal{B}(\tau^- \rightarrow K^-\pi^0\nu_\tau) = \frac{1}{2N_{\tau\tau}} \frac{N_{\text{data}} - N_{\text{bkg}}}{\varepsilon_{\text{sig}}}, \quad (4)$$

where  $N_{\tau\tau}$  is the total number of  $\tau^+\tau^-$  pairs in the real data,  $N_{\text{data}}$  is the number of selected events in real data,  $N_{\text{bkg}}$  is the number of background events estimated from Monte Carlo. The total number of  $\tau^+\tau^-$  pairs in the data is given by:

$$N_{\tau\tau} = \sigma_\tau \mathcal{L}_{\text{data}} = 110\,683\,856, \quad (5)$$

where  $\sigma_\tau$  is the  $\tau^+\tau^-$  production cross-section at *BABAR* (i.e. 0.89 nb) and  $\mathcal{L}_{\text{data}}$  is the (integrated) real data luminosity (i.e.  $124.4\text{fb}^{-1}$ ).  $N_{\tau\tau}$  is subject to correlated uncertainties from the cross-section and luminosity, as discussed in Section 5.

Table 2 gives the numbers of real and simulated data events passing the selection criteria that feed into the  $\mathcal{B}(\tau^- \rightarrow K^-\pi^0\nu_\tau)$  calculation. A preliminary result for the measurement of the branching fraction  $\mathcal{B}(\tau^- \rightarrow K^-\pi^0\nu_\tau)$  is given in Table 3. Figure 2 shows that our result is the world's most precise measurement of  $\mathcal{B}(\tau^- \rightarrow K^-\pi^0\nu_\tau)$  to date and it is consistent with the current world average [10].

Table 2

Numbers of real and Monte Carlo data events remaining in the selected samples corresponding to the  $124.4\text{fb}^{-1}$  (integrated) real data luminosity.

Data	$e$ -tag	$\mu$ -tag	Combined
Real	$12377 \pm 111$	$9301 \pm 96$	$21678 \pm 147$
$\tau^+\tau^-$	$3494 \pm 59$	$2512 \pm 50$	$6006 \pm 78$
$uds$	$25 \pm 5$	$48 \pm 6$	$73 \pm 8$
$c\bar{c}$	$5 \pm 2$	$2 \pm 1$	$7 \pm 2$
$B\bar{B}$	-	-	-

Table 3

$\mathcal{B}(\tau^- \rightarrow K^-\pi^0\nu_\tau)$  measured in this analysis.

Sample	$\mathcal{B}(\tau^- \rightarrow K^-\pi^0\nu_\tau)$ [%]
$e$ -tag	$0.436 \pm 0.005$ (stat) $\pm 0.022$ (syst)
$\mu$ -tag	$0.442 \pm 0.006$ (stat) $\pm 0.025$ (syst)
Combined	$0.438 \pm 0.004$ (stat) $\pm 0.022$ (syst)

## 7. SUMMARY

Using  $124.4\text{fb}^{-1}$  of  $e^+e^-$  collision data produced by the PEP-II accelerator and recorded by the *BABAR* detector, we obtain the preliminary result:

$$\mathcal{B}(\tau^- \rightarrow K^-\pi^0\nu_\tau) = (0.438 \pm 0.004 \text{ (stat)} \pm 0.022 \text{ (syst)}) \%. \quad (6)$$

This result is the world's most precise measurement of this branching fraction to date and is consistent with the world average.

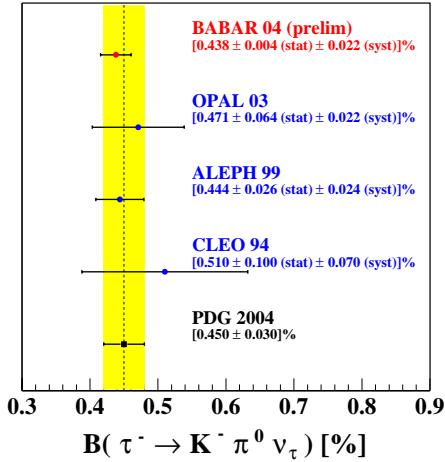


Figure 2. World measurements of  $\mathcal{B}(\tau^- \rightarrow K^- \pi^0 \nu_\tau)$ . This analysis provides the world's most precise measurement to date:  $\mathcal{B}(\tau^- \rightarrow K^- \pi^0 \nu_\tau) = (0.438 \pm 0.004 \text{ (stat)} \pm 0.022 \text{ (syst)}) \%$ .

## 8. ACKNOWLEDGEMENTS

We are grateful for the extraordinary contributions of our PEP-II colleagues in achieving the excellent luminosity and machine conditions that have made this work possible. The success of this project also relies critically on the expertise and dedication of the computing organizations that support *BABAR*. The collaborating institutions wish to thank SLAC for its support and the kind hospitality extended to them. This work is supported by the US Department of Energy and National Science Foundation, the Natural Sciences and Engineering Research Council (Canada), Institute of High Energy Physics (China), the Commissariat à l'Energie Atomique and Institut National de Physique Nucléaire et de Physique des Particules (France), the Bundesministerium für Bildung und Forschung and Deutsche Forschungsgemeinschaft (Germany), the Istituto Nazionale di Fisica Nucleare (Italy), the Foundation for Fundamental Research on Matter (The Nether-

lands), the Research Council of Norway, the Ministry of Science and Technology of the Russian Federation, and the Particle Physics and Astronomy Research Council (United Kingdom). Individuals have received support from CONACyT (Mexico), the A. P. Sloan Foundation, the Research Corporation, and the Alexander von Humboldt Foundation.

## REFERENCES

1. E. Gamiz *et al.*, JHEP 0301 (2003) 060.
2. S. Chen *et al.*, Eur. Phys. J. C22 (2001) 31.
3. R. Briere *et al.*, Phys. Rev. Lett. 90 (2003) 181802.
4. G. Abbiendi *et al.*, Eur. Phys. J. C35 (2004) 437.
5. B. Aubert *et al.*, Nucl. Instrum. Meth. A479 (2002) 1.
6. PEP-II: An asymmetric *B* Factory. Conceptual Design Report, 1993, SLAC-R-418.
7. B.F.L. Ward, S. Jadach and Z. Was, Nucl. Phys. Proc. Suppl. (2003) 73.
8. S. Jadach, Z. Was R. Decker and J.H. Kühn, Comput. Phys. Commun. 76 (1993) 361.
9. K. Hagiwara *et al.*, Phys. Rev. D66 (2002) 010001.
10. S. Eidelman *et al.*, Phys. Lett. B592 (2004) 1.